ISSN 1330-3651 (Print), ISSN 1848-6339 (Online)
https://doi.org/10.17559/TV-20240122001282
Original scientific paper

Miniaturised Wide and Dual band Reconfigurable Antenna on-demand for Portable Wireless Devices

G. JANSIRANI*, R. GANDHI RAJ

Abstract: This article presents a compact reconfigurable antenna capable of wide-band, dual-band operation. The proposed antenna is having two closed rings with ELC integration in the inner ring. The entire structure is designed and fabricated on a FR4 substrate with the foot print area of 30 × 31 mm². Initially, a circular ELC-based monopole antenna operating within the frequency range of 2.4 - 2.7 GHz is described. By integrating two p-i-n diodes between the rings and ELC, distinct operating frequency bands are achieved through toggling the diodes. With one diode active, the antenna functions at 2.4 - 2.7 GHz and 4.2 - 4.3 GHz. Activating both diodes extends the bandwidth, enabling operation within the same frequency ranges. The bandwidth of 3200 and 98 MHz is achived in both the bands respectiveley. The gain of the proposed antenna is maintained above 2.0 dBi in the entire operating frequency range. The antenna's compact design, suitable for WiMAX and WLAN applications, is emphasized, and a comparison with contemporary designs underscores its size efficiency and versatile operational modes.

Keywords: PIN diode; printed antenna; reconfigurable antenna; WiMAX; WLAN

1 INTRODUCTION

In recent years, the commercial growth of 5G networks urged the demand for dual-band, and multiband functional antennas [1, 2]. Being the commercial network, the cellular and mobile technologies are depending on the standards such as Wi-fi, Wi-Max, WLAN, and GPS, considered to be the important standards in mobile communication networks. The aforementioned standards require portable and efficient small-sized antennas which could operate at multiple frequencies simultaneously. Multiband functional antennas present themselves to be a key component for such mobile applications, which are modelled with different configurations for achieving the mentioned multiband functionality [3-5]. Planar antennas found themselves useful in implementing such multi-band antennas due to their distinct and appealing behaviour to fulfil the developing network's requirement [6, 7]. Microstrip patch/planar antennas have become popular in today's communication systems because of their obvious advantages such as low production costs, lightweight, low-profile configurations, and easy integration with active and passive electronic circuitry [8-10]. However the modelled antennas for such applications occupy a larger volume which makes it difficult to embed in compact devices (dual band antenna). Miniaturization has become critical for optimal design. There are numerous antenna miniaturisation techniques, all of which involve a trade-off between size and performance (bandwidth and/or radiation yield), such as charging by passive elements, short circuit application, slots insertion, and the use of a dielectric substrate with extremely high permittivity and meta-materials [11]. Doubly negative materials (DNG) or meta-materials are materials with negative constitutive parameters such as negative permittivity (ε) and permeability (μ). These materials have never been found in nature and must be obtained artificially.

2 LITERATURE SURVEY

Because of their unprecedented electromagnetic properties, metamaterial [17-26] inspired antennas are critical for improving antenna performance. Many antenna designers have pushed metamaterial-inspired structures to improve antenna performance. To build microwave components, a complementary split ring resonator (CSRR)-based metamaterial was created [12-14]. Image rejection in RF down-converters [15], reduction of side lobe level [16], gain improvement, good impedance matching [17], and multiband antenna design [18] are all possible with CSRR-based artificial materials. The negative permittivity based CSRR metamaterial provides circular polarisation while reducing cross polarisation [19, 20]. The CSRR embedded monopole achieved a new resonance frequency as well as antenna miniaturisation at the same time [21]. The concept of reconfigurable antennas have garnered significant interest in wireless communication and IoT research due to their ability to operate across various frequency bands on a single platform . These antennas, as patented by Schaubert et al., adjust their operating frequency, impedance bandwidth, radiation pattern, and polarization to meet the requirements of the host system . Hybrid structures of reconfigurable antennas modify multiple performance parameters, offering cost, weight, and volume savings. Three switching mechanisms-electrical, mechanical, and optical-are commonly employed in their design . Electrical switching utilizes RF switches like PIN diodes and MEMS for discrete tuning, while varactor diodes enable continuous frequency tuning [22]. Mechanical switching employs tunable materials such as liquid crystals and metasurfaces for frequency agility, whereas optically controlled frequency reconfigurable antennas utilize optical waveguides or photonic crystals to adjust resonant frequencies. A notable example is frequency reconfigurable multiband antenna design for microwave sensing applications [23]. This design, utilizing PIN diodes, switches the operating frequency.

3 MATERIALS AND METHODS

On a substrate made of FR4 with a dielectric constant of 4.4 and a loss tangent of 0.002, the triband ELC antenna that has been proposed can be built. In order to get at the proposed antenna, there are four stages of design. As a seed antenna, we use a straightforward circular monopole that is

designed to function at a frequency of 2.5 GHz. In order to create the proposed antenna, a circular ring needs to be carved, and ELC must be incorporated into the seed antenna. Electrically speaking, the suggested antenna has dimensions of 36 millimetres by 31 millimetres by 1.6 millimetres (0.3 microns by 0.26 microns by 0.0133 microns). The suggested antenna has a dual band operation with a bandwidth of 330 MHz and 120 MHz. The operating frequency band of the proposed antenna is from 2.4 - 2.7 GHz, and 4.2 - 4.3 GHz. It also includes resonances at 2.5 GHz, and 4.3 GHz, making it appropriate for use in WIMAX, and WLAN, applications. The designs of the proposed antennas, antenna 1, antenna 2, and antenna 3, are the stages of the design process for the triband ELC antenna. Antenna 1 is a straightforward circular disc antenna with a ground dimension of $W \times Lg$. It has a radius of 8 millimetres and is fed by a microstrip wire with a resistance of 50 ohms. Etching a circular ring with 7 mm as the outer ring radius and 6 mm as the inner ring radius, respectively, is used in the design . Etching another circular ring with a radius of 5 mm is used, and finally, the intended to ELC antenna is designed by using the ELC structure as an inner ring.

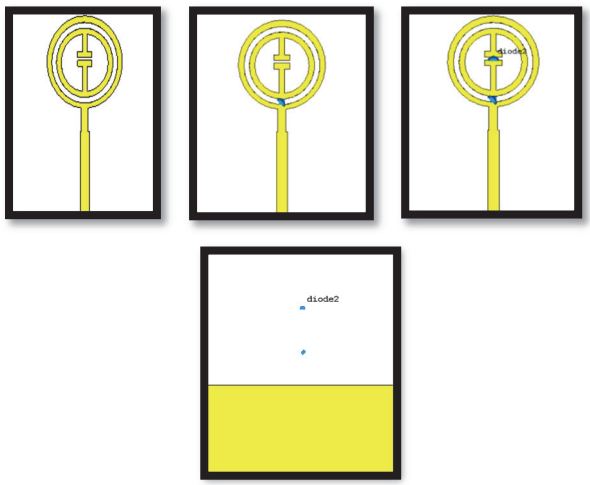

Figure 1 Evolution of the proposed antenna

Fig. 1 illustrates the proposed antenna's four different design stages, showing both the front and the back views. The suggested triband ELC antenna's geometric design can be seen illustrated in Fig. 2, and the parameter values for the antenna can be found in Tab. 1.

Fig. 2 shows the seed antenna without PIN diode. The proposed structure operates at one frequency at 2.4 - 2.7 GHz. The return loss plot of the stage 1 of the proposed antenna is presented in Fig. 2. Two p-i-n diodes connect between the rings and ELC respectively. Switching these p-i-n diodes on and off creates distinct operating frequency bands. The antenna operates at 2.4 - 2.7 GHz, and 4.2 - 4.3 GHz with one diode. The antenna with single diode between the inner and outer ring is presented in Fig. 4 and its return loss plots are presented in Fig. 5. When both p-i-n diodes are ON, the antenna may operate from 2.4 - 2.7 GHz, and 4.2 - 4.3 GHz with increased bandwidth. The antenna with two diodes is presented in Fig. 6 and its return loss comparison for various ON and OFF states is presented in Fig. 7.

Table 1 Parameters Values (IN MM)

L	*W*	*WF*	*LF*	*L*1	*W*1	*S*
30	31	1	10	3	1	1
*L*2	*R*1	*R*2	*a*	*L*3	*X*	*Y*
7	7	6	0.5	2	0.5	2

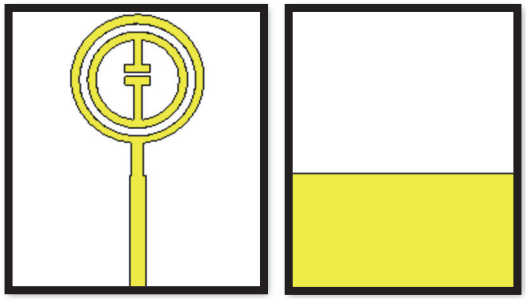

Figure 2 Proposed ELC antenna stage 1

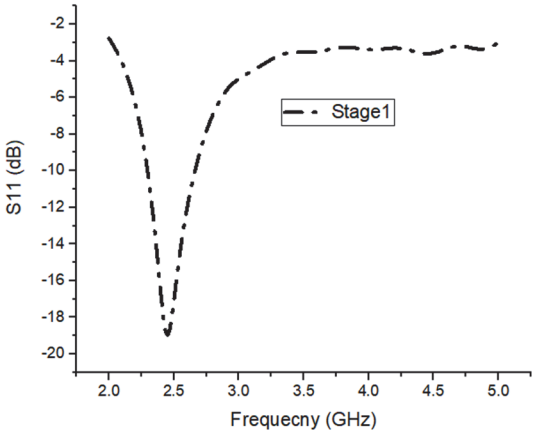

Figure 3 S11 plot of stage 1

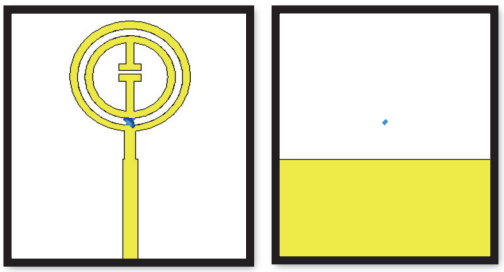

Figure 4 Stage 2 Proposed ELC with Single diode

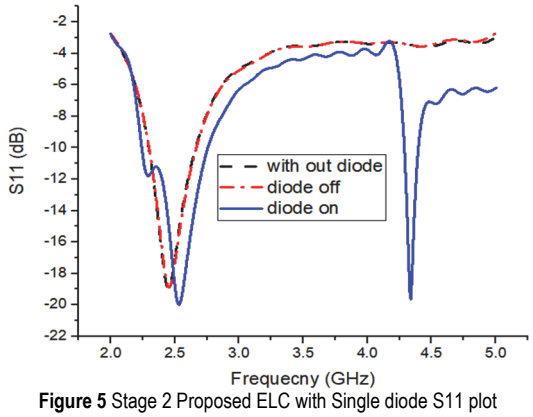

Figure 5 Stage 2 Proposed ELC with Single diode S11 plot

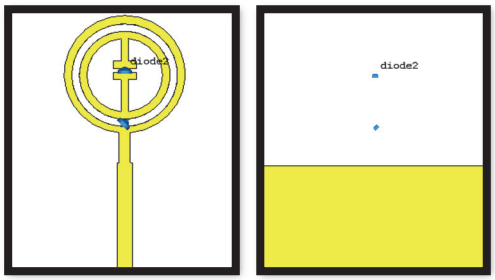

Figure 6 Stage 3 Proposed ELC with dual diode

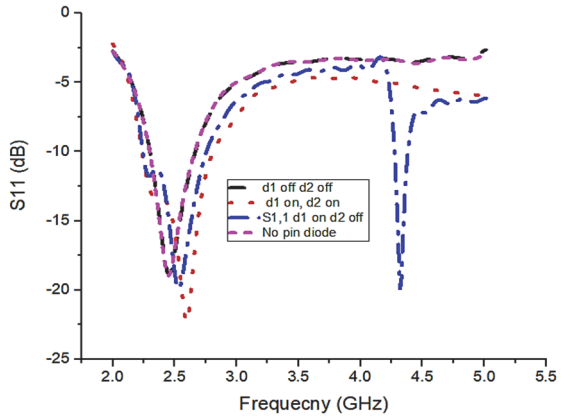

Figure 7 Stage 3 proposed ELC with dual diode s11 comparison plot

4 EVOLUTION AND DESIGN

We study the effect that ground length (Lg), gap spacing between the rings (a), and ELC capacitive gap (x) have on return loss by utilising the parametric research capabilities of the CST programme. More specifically, our attention is focused on these three aspects. The ground length (Lg) is increased by 0.8 mm at a time, taking it from 14 mm all the way up to 15.6 mm in total length. Because using Lg = 14.8 mm results in correct impedance matching being achieved across the board for all of the resonating bands, this dimension has been settled on as the one to utilise for the final construction. The influence that Lg has on the amount of return loss that takes place is depicted in Fig. 8a. After that, the space in between the rings is stretched out to 1.2 millimetres, up from 0.8 millimetres, using increments of 0.2 millimetres each time. Because of this, there is a change in the 2.3 GHz band, which demonstrates that the inner ring is the factor responsible for the shift. As can be seen in Fig. 8(b), a value of a = 1 mm achieves impedance matching that is both complete and reasonable for the 2.3 GHz band. This is the case for both of the other bands as well. As a consequence of this, the value will be the one that is applied in the end. The adjustment made to the value of X does not affect the lower resonating frequency in any way, but it does have a considerable effect on the resonating band that is generated by the ELC. The resonant frequency can be seen to decrease as the capacitive gap gets smaller in Fig. 8(c), and it can be shown that the resonant frequency can increase as the capacitive gap gets larger. Both of these results may be seen. You can determine this information by comparing the two different figures. Because x = 1 millimetre provides us with the WAIC band that we want, we employ it in the production process for the final product. The parametric study that was conducted on X makes it quite clear that the presence of the ELC structure in the proposed antenna is the root cause of the band that operates at 4.3 GHz. This conclusion was reached as a result of the study.

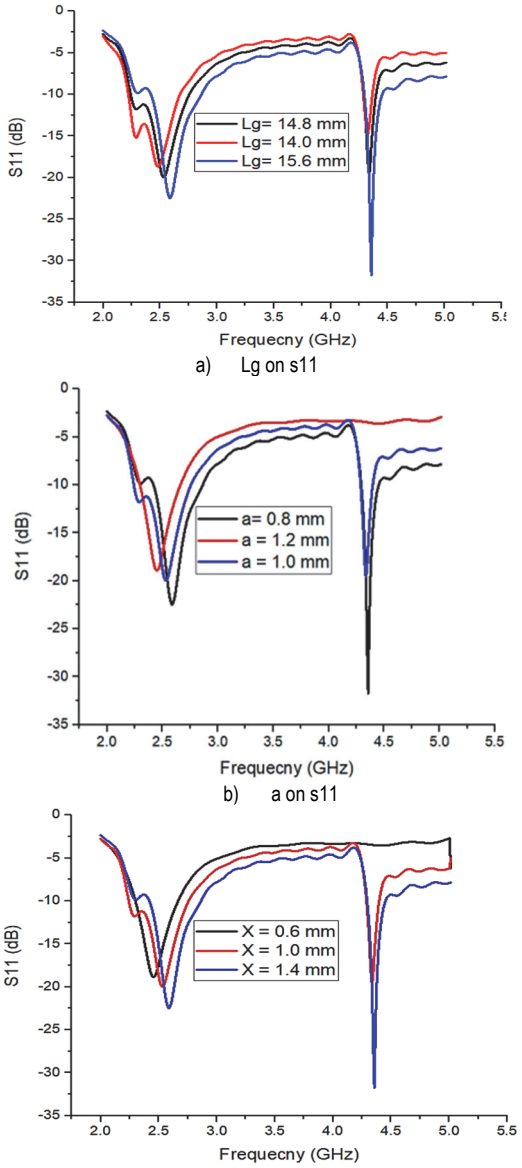

Figure 8 Parametric analysis

5 RESULTS AND DISCUSSION

Fig. 9 displays the simulated surface current distribution for frequencies of 2.5 GHz, and 4.3 GHz respectively.

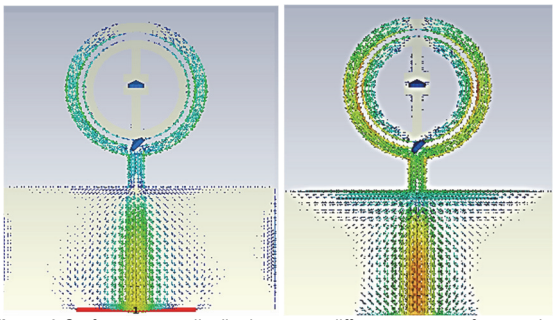

Figure 9 Surface current distribution at two different resonant frequencies

It has been discovered that the highest current may be found centred around the circular rings in the lower band, as well as at the ELC structure in the band operating at 4.31 GHz. The existing distribution makes it quite clear that the ring and ELC are responsible for the proposed antenna's bands. Fig. 6 reveals that the ELC is operating at 4.31 GHz, as measured by its resonance frequency. Because of this, the permeability supplied by the ELC is negative at this frequency, which complies with the metamaterial properties; as a result, it is the factor that is responsible for the resonance at 4.31 GHz. In each of the resonant frequency bands, a dipole pattern in the E plane with the shape of an eight and an omnidirectional pattern in the H plane is obtained. The radiation patterns that were measured and those that were simulated are both displayed in Fig. 10, and there is a high degree of congruence between the two. The antenna's stability and reliability during frequency band switching are ensured through rigorous testing protocols, confirming consistent performance across all operating frequencies. Additionally, extensive simulations and real-world experimentation validate the antenna's robustness and durability under varying frequency conditions.

A comparison of the results obtained through measurement and those obtained through simulation is shown in Tab. 2. The influence of fabrication and soldering is the cause of the tiny discrepancy that may be seen between the simulated and measured results. Fig. 11 represents the directivity, and it is observed from the figure that directivity is maintained above2 dBi in the entire operating region. Fig. 12 presents a comparison of the simulated gain with the measured gain. At 2.5 GHz, and 4.3 GHz, respectively, the highest gain was measured at 3.2, and 4.1 dBi. In Fig. 13, the fabricated antenna is presented. The comparison graph between the measured and simulated results is presented in Fig. 14. The disagreement between the results is due to the fabrication and measurement errors.

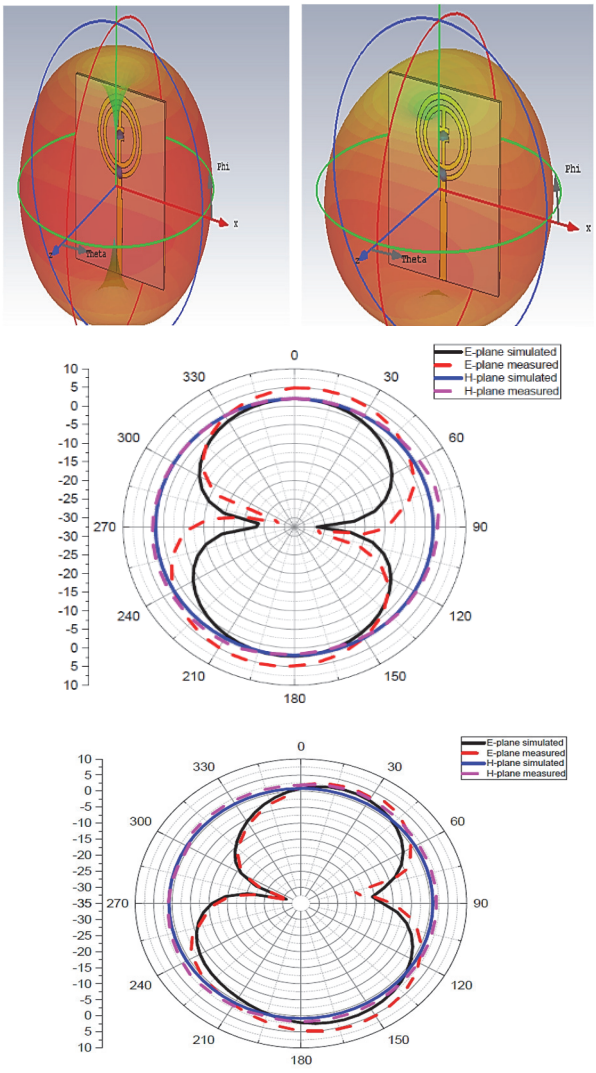

Figure 10 Radiation pattern measurement at two different resonating frequencies

Table 2 Simulated and Measured Result Comparison of Elc Triband Antenna

ELC Triband Antenna							
Simulated Result				Measured Result			
Centre Frequency / GHz	Return Loss / dB	Operating Band / GHz	Impedance Bandwidth / MHz	Centre Frequency / GHz	Return Loss / dB	Operating Band / GHz	Impedance Bandwidth / MHz
2.5	–20.9	2.4 to 2.7	3100	2.7	–23.17	2.3 to 2.9	3200
4.3	–29.5	4.1 to 4.3	110	4.37	–19.81	4.33 to 4.42	98

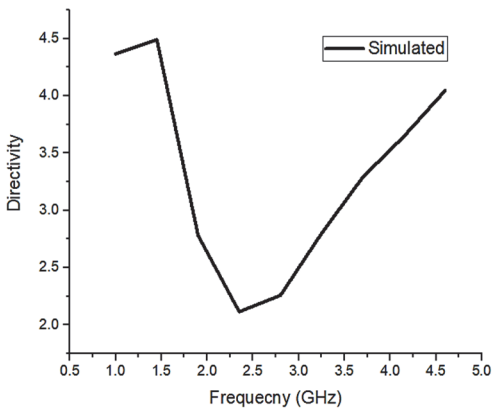

Figure 11 Directivity vs frequency

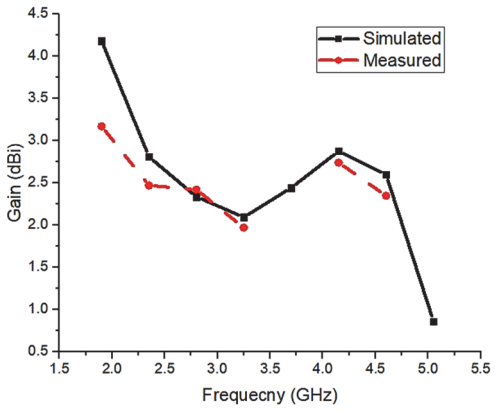

Figure 12 Gain vs frequency

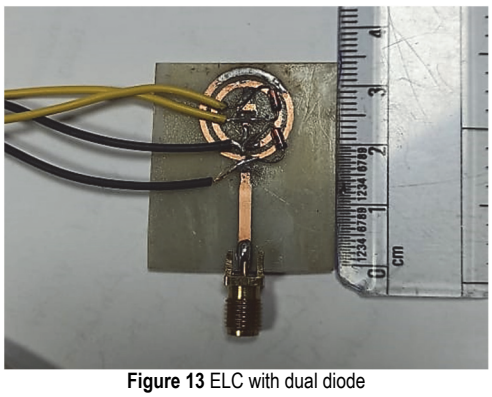

Figure 13 ELC with dual diode

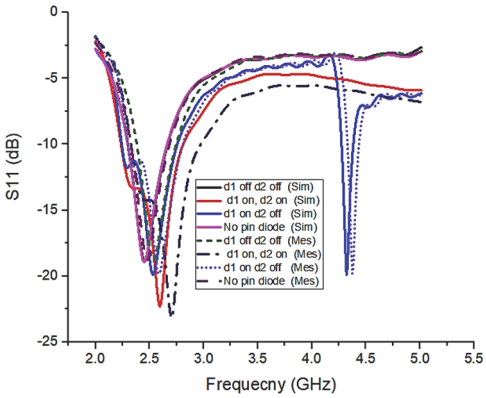

Figure 14 Measured vs simulated s11 characteristics

6 CONCLUSION AND FUTURE SCOPE

Circular ELC metamaterial triband antennas for WIMAX, and WLAN, have been proposed. ELC structure in the circular radiating element achieves tri-band. Gain and radiation patterns match the simulated results. Gain and loss are measured. A parametric examination of the essential factors and how they affect antenna performance is also provided. The suggested ELC metamaterial element's negative permeability is at 4.2 GHz. The outer ring 2.4 to 2.9 GHz, and the ELC 4.1 to 4.4 GHz. Simulation and equations show this. Due to its simplicity, size, triband capabilities, and symmetric emission pattern, the suggested antenna's proposed structure can be integrated with EBG structures and Reflectors to enhance the gain and directivity.

7 REFERENCES

[1] Ullah, S., Ahmad, S., Khan, B. A., & Flint, J. A. (2018). A multi-band switchable antenna for Wi-Fi, 3G Advanced, WiMAX, and WLAN wireless applications. *International Journal of Microwave and Wireless Technologies, 10*(8), 991-997. https://doi.org/10.1017/S1759078718000776

[2] Thiruvenkadam, S. & Parthasarathy, E. (2023). Compact multiband monopole antenna design for IoT applications. *Journal of Electromagnetic Waves and Applications, 37*(5), 629-643. https://doi.org/10.1080/09205071.2022.2163191

[3] Aliqab, K., Lavadiya, S., Alsharari, M., Armghan, A., Daher, M. G., & Patel, S. K. (2023). Design and Fabrication of a Low-Cost, Multiband and High Gain Square Tooth-Enabled Metamaterial Superstrate Microstrip Patch Antenna. *Micromachines, 14*(1), 163. https://doi.org/10.3390/mi14010163

[4] Islam, T. & Roy, S. (2023). Low-Profile Meander Line Multiband Antenna for Wireless Body Area Network (WBAN) Applications with SAR Analysis. *Electronics, 12*(6), 1416. https://doi.org/10.3390/electronics12061416

[5] Dakulagi, V. & Bakhar, M. (2020). Advances in smart antenna systems for wireless communication. *Wireless Personal Communications, 110*(2), 931-957. https://doi.org/10.1007/s11277-019-06764-6

[6] Kumar, A. & Al-Hasan, M. A. J. (2020). A coplanar-waveguide-fed planar integrated cavity backed slotted antenna array using TE33 mode. *International Journal of RF and Microwave Computer-Aided Engineering, 30*(10), e22344. https://doi.org/10.1002/mmce.22344

[7] Kumar, A. & Althuwayb, A. A. (2020). Wideband triple resonance patch antenna for 5G Wi-Fi spectrum. *Progress in Electromagnetics Research Letters, 93*, 89-97. https://doi.org/10.2528/PIERL20071605

[8] Kristou, N. (2018). *Étude et conception de métamatériaux accordables pour la miniaturisation d'antennes aux fréquences micro-ondes*. Doctoral dissertation, University of Rennes.

[9] Kumar, K. P. & Karthikeyan, S. S. (2015). Wideband three section branch line coupler using triple open complementary split ring resonator and open stubs. *AEU-International Journal of Electronics and Communications, 69*(10), 1412-1416. https://doi.org/10.1016/j.aeue.2015.06.003

[10] Sam, P. J. C. & Gunavathi, N. (2020). A tri-band monopole antenna loaded with circular electric-inductive-capacitive metamaterial resonator for wireless application. *Applied Physics A, 126*, 774. https://doi.org/10.1007/s00339-020-03952-1

[11] Lakshmi, M. L. S. N. S., Prasad Jones Christydass, S., Kannadhasan, S., Anguraj, K., & Chatterjee, J. M. (2023). Polarization Stable Triband Thin Square-Shaped Metamaterial Absorber. *International Journal of Antennas and Propagation, 2023*, 6065300. https://doi.org/10.1155/2023/6065300

[12] Goswami, S., Sarmah, K., Sarma, A., Sarma, K. K., & Baruah, S. (2017). Design of a CSRR based compact microstrip antenna for image rejection in RF down-converter based WLAN receivers. *AEU-International Journal of Electronics and Communications, 74*, 128-134. https://doi.org/10.1016/j.aeue.2017.02.004

[13] Wahid, A., Sreenivasan, M., & Rao, P. H. (2015). CSRR loaded microstrip array antenna with low sidelobe level. *IEEE Antennas and Wireless Propagation Letters, 14*, 1169-1171. https://doi.org/10.1109/LAWP.2015.2396084

[14] Pandeeswari, R. & Raghavan, S. (2015). Microstrip antenna with complementary split ring resonator loaded ground plane for gain enhancement. *Microwave and Optical Technology Letters, 57*(2), 292-296. https://doi.org/10.1002/mop.28835

[15] Christydass, S. P. J. & Gunavathi, N. (2021). Dual-band complementary split-ring resonator engraved rectangular monopole for GSM and WLAN/WiMAX/5G sub-6 GHz band (new radio band). *Progress in Electromagnetics Research C, 113*, 251-263. https://doi.org/10.2528/PIERC21052007

[16] Mehdipour, A., Denidni, T. A., & Sebak, A. R. (2013). Multi-band miniaturized antenna loaded by ZOR and CSRR metamaterial structures with monopolar radiation pattern. *IEEE Transactions on Antennas and Propagation, 62*(2), 555-562. https://doi.org/10.1109/TAP.2013.2290791

[17] Christydass, S. P. J. & Gunavathi, N. (2021). Octa-Band Metamaterial Inspired Multiband Monopole Antenna for Wireless Application. *Progress in Electromagnetics Research C, 113*, 97-110. https://doi.org/10.2528/PIERC21041102

[18] Boopathi Rani, R. & Pandey, S. K. (2017). ELC metamaterial based CPW-fed printed dual-band antenna. *Microwave and optical technology letters, 59*(2), 304-307. https://doi.org/10.1002/mop.30292

[19] Liu, X. Y., Wu, Z. T., Fan, Y., & Tentzeris, E. M. (2016). A miniaturized CSRR loaded wide-beam width circularly polarized implantable antenna for subcutaneous real-time glucose monitoring. *IEEE Antennas and Wireless Propagation Letters, 16*, 577-580. https://doi.org/10.1109/LAWP.2016.2590477

[20] Roja, G., Maheswara Venkatesh, P., & Jayasankar, T. (2023). Split Ring Resonator Inspired Dual-Band Monopole Antenna for ISM, WLAN, WIFI, and WiMAX Application. *Technical Gazette, 30*(5), 1533-1538. https://doi.org/10.17559/TV-20230210000344

[21] Çalışır, B. & Akbal, A. (2022). A New RF Satellite Link Analyzing and Antenna Effect on Satellite Communication. *Tehnički glasnik, 16*(4), 550-556. https://doi.org/10.31803/tg-20220405153200

[22] Ermiş, S. & Demirci, M. (2023). Improving the Performance of Patch Antenna by Applying Bandwidth Enhancement Techniques for 5G Applications. *Tehnički glasnik, 17*(3), 305-312. https://doi.org/10.31803/tg-20220819001236

[23] Prasad Jones Christydass, S., Suresh Kumar, S., Nishok, V. S., Saravanakumar, R., Devakirubakaran, S., Deepa, J., & Sangeetha, K. (2023). Design of Metamaterial Antenna Based on the Mathematical Formulation of Patch Antenna for Wireless Application. *International Journal of Antennas and Propagation, 2023*, 2543923. https://doi.org/10.1155/2023/2543923

Contact information:

G. JANSIRANI
(Corresponding author)
Department of Electrical and Electronics Engineering,
University College of Engineering (BIT Campus), Anna University,
Tiruchirappalli, Tamil Nadu, India
E-mail: g.jansirani@rediffmail.com

R. GANDHI RAJ
Department of Electrical and Electronics Engineering,
University College of Engineering (BIT Campus), Anna University,
Tiruchirappalli, Tamil Nadu, India
E-mail: gandhirajeee@gmail.com